ELSEVIER

Purification of beet molasses by ion-exclusion chromatography: fixed-bed modelling

Marie-Laure Lameloise*, Richard Lewandowski

ENSIA (Ecole Nationale Supérieure des Industries Agricoles et Alimentaires), 1 avenue des Olympiades, 91305 Massy, France

Abstract

Sucrose recovery from beet molasses was studied by ion-exclusion chromatography. On the basis of sucrose and NaCl adsorption isotherms, a simple equilibrium model was computed that gave good agreement with molasses band profiles on a single column. At high concentration, it was found necessary to introduce mass transfer resistance to account for band broadening.

1. Introduction

Molasses is a by-product of the sugar industry that still contains about 50% of sucrose. The current development of continuous chromatographic processes [simulated moving bed (SMB)] has given a new impetus to molasses desugarization by ion exclusion in countries where sucrose recovery is economically or technically justified. Many process suppliers have proposed continuous systems for molasses purification and have already built some plants [1–4]. However, very little information is available about the optimum design method, procedural strategy and performance. Optimization of a SMB system requires modelling. The first step consists in modelling the separation on a single column.

Industrial plants involving the SMB principle (about 100 according to Hotier [5]) process purified mixtures, often containing not more than two or three well identified compounds; an

example in the food industry is the extensively studied glucose–fructose separation. Actually, most current or potential applications of preparative chromatography in the food industry concern inputs having complex and often variable compositions, as illustrated in Table 1 for molasses. If the principle of molasses purification is based on Donnan exclusion of ionic species together with a weak adsorption of sucrose, other phenomena may take place to some extent. Modelling of such complex systems requires appropriate methodology.

Most studies addressing preparative-scale chromatographic modelling have dealt with separations in which compounds exhibit favourable, generally Langmuir-type, equilibrium isotherms. Now, ion-exclusion isotherms are well known to be unfavourable and those interested in applications of ion exclusion, whatever the field, have generally not tried to model them. Working on cane molasses desugarization, Saska et al. [7] were one of the very few groups to propose a model including a mathematical representation

* Corresponding author.

Table 1
Typical beet molasses composition (from Ref. [6])

Component	Content (g per 100 g)
Dry matter	75
Total sugar	48–52
Sucrose	48–52
Glucose/fructose	0.2–1.2
Raffinose	0.5–2
Organic matter	12–17
Nitrogeneous	6–10
Non-nitrogeneous	6–7
Mineral matter	10–12
Sodium	0.3–0.7
Potassium	2–7
Calcium	0.1–0.5
Chloride	0.5–1.5
Phosphorus	0.02–0.07

Fig. 1. Equilibrium isotherms of sucrose in mixtures with NaCl at various concentrations: $\bigcirc = 0$; $\bullet = 42$; $+ = 75$; $\boxtimes = 110$ g/l. Conditions: 70°C on Dowex C326 resin (from [8]).

Fig. 2. Equilibrium isotherms of NaCl in mixtures with sucrose at various concentrations: $\bigcirc = 0$; $\bullet = 98$; $\blacktriangle = 292$; $\boxtimes = 483$ g/l. Conditions: 70°C on Dowex C326 resin (from [8]).

of unfavourable isotherms; however, owing to the non-linearity, a simplified version had to be derived to allow easy simulation of SMB purification.

The methodology we decided to adopt in this study has been detailed in a previous publication [8]: molasses is assimilated to a binary mixture containing sucrose and a salt; as resin used for molasses desugarization is generally in the Na^+ form (at least at the beginning) NaCl is selected as the salt and its concentration is taken as equal to that of the ash, representative of ionic-excluded compounds in molasses. Sucrose and NaCl adsorption isotherms have been measured by frontal analysis on single compounds and on mixtures in a broad range of concentrations (up to nearly 600 g/l for sucrose and 110 g/l for NaCl) and found to be unfavourable and interdependent (Figs. 1 and 2). A second-order polynomial was found convenient to represent each set of isotherms, with appropriate coefficients:

Sucrose:
$$q_1 = 0.167c_1 + 0.307 \cdot 10^{-3}c_1^2 + 0.172 \cdot 10^{-2}c_1c_2$$
NaCl:
$$q_2 = 0.068c_2 + 0.176 \cdot 10^{-2}c_2^2 + 0.293 \cdot 10^{-3}c_2c_1$$

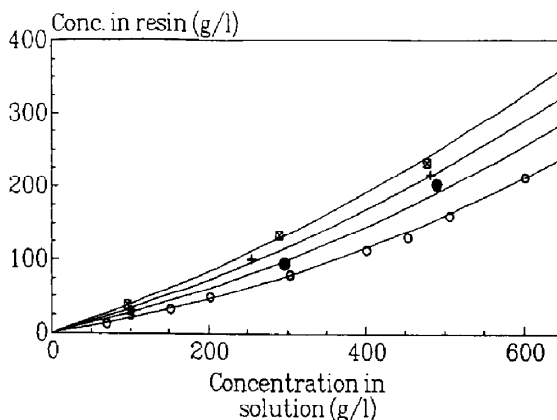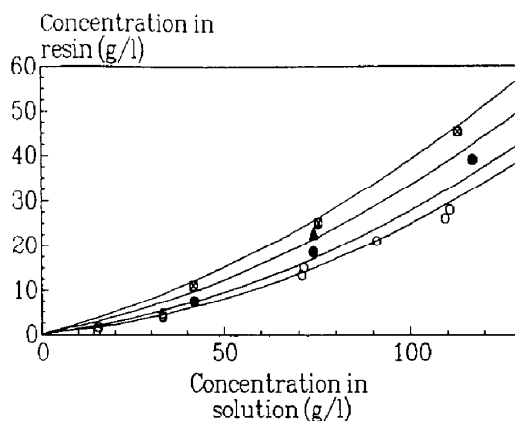As equilibrium data play the major role in shaping the band profiles, a simple equilibrium

model based on previously measured isotherms is now computed to simulate the experimental elution of molasses.

2. Simple equilibrium model

This model is described by the following equations:

Mass balance in the liquid phase for the two solutes:

Sucrose:

$$u \cdot \frac{\partial c_1}{\partial z} + \frac{\partial c_1}{\partial t} + \frac{(1-\varepsilon)}{\varepsilon} \cdot \frac{\partial q_1}{\partial t} = 0 \qquad (1)$$

NaCl:

$$u \cdot \frac{\partial c_2}{\partial z} + \frac{\partial c_2}{\partial t} + \frac{(1-\varepsilon)}{\varepsilon} \cdot \frac{\partial q_2}{\partial t} = 0 \qquad (2)$$

Equilibrium isotherms:
Sucrose:

$$q_1 = ac_1 + bc_1^2 + dc_1c_2 \qquad (3)$$

NaCl:

$$q_2 = a'c_2 + b'c_2^2 + d'c_1c_2 \qquad (4)$$

Using normalized coordinates $[x = z/L$ and $\tau = t/t_0 = t(u/L)]$, the following set of equations is obtained:

$$\frac{\partial c_1}{\partial x} + A \cdot \frac{\partial c_1}{\partial \tau} + B \cdot \frac{\partial c_2}{\partial \tau} = 0 \qquad (5)$$

$$\frac{\partial c_2}{\partial x} + A' \cdot \frac{\partial c_2}{\partial \tau} + B' \cdot \frac{\partial c_1}{\partial \tau} = 0 \qquad (6)$$

A, A', B and B' depend on c_1 and c_2.

Numerical solution of this set of partial differential equations cannot be achieved by Laplace or Fourier transform methods, because of the nonlinearity of the isotherms. Resolution with a finite difference method was undertaken.

Time derivatives are calculated at $(x, \tau + \Delta\tau/2)$ and a second-order Crank–Nicolson scheme is applied:

$$\left.\frac{\partial c}{\partial \tau}\right|_{x,\tau+\Delta\tau/2} = \frac{c(x,\tau+\Delta\tau) - c(x,\tau)}{\Delta\tau} \qquad (7)$$

For space derivatives, a first-order backward difference is applied:

$$\left.\frac{\partial c}{\partial x}\right|_{x,\tau+\Delta\tau/2} = \frac{1}{2} \cdot \left.\frac{\partial c}{\partial x}\right|_{x,\tau} + \frac{1}{2} \cdot \left.\frac{\partial c}{\partial x}\right|_{x,\tau+\Delta\tau} \qquad (8)$$

$$= \frac{1}{2} \cdot \frac{[c(x,\tau) - c(x-\Delta x,\tau) + c(x,\tau+\Delta\tau) - c(x-\Delta x,\tau+\Delta\tau)]}{\Delta x}$$

with the following approximations:

$$c_1(x, \tau + \Delta\tau/2) = c_1(x, \tau) \qquad (9)$$

$$c_2(x, \tau + \Delta\tau/2) = c_2(x, \tau) \qquad (10)$$

The set of Eqs. 5 and 6 becomes a simple linear system of two equations with two unknowns:

$$c_1(x, \tau + \Delta\tau)P + c_2(x, \tau + \Delta\tau)Q + R = 0 \qquad (11)$$

$$c_2(x, \tau + \Delta\tau)P' + c_1(x, \tau + \Delta\tau)Q' + R' = 0 \qquad (12)$$

Given initial and boundary conditions, iterative calculation allows the column response $c_1(1, \tau)$ and $c_2(1, \tau)$ to be readily obtained.

For a rectangular injection of concentration c_1^0 in sucrose and c_2^0 in NaCl and of normalized duration τ_e, the initial conditions are expressed as follows:

$$0 < \tau \leqslant \tau_c \quad c_1(0, \tau) = c_1^0 \quad c_2(0, \tau) = c_2^0 \qquad (13)$$

$$\tau > \tau_c \qquad c_1(0, \tau) = 0 \quad c_2(0, \tau) = 0 \qquad (14)$$

$$\tau = 0 \qquad c_1(x, 0) = 0 \quad c_2(x, 0) = 0 \qquad (15)$$

A proper choice of time and space increments $\Delta\tau$ and Δx has to be made to ensure stability and precision of the result; in practice, we have found that $\Delta\tau = 0.007$ and $\Delta x = 0.0025$ gave a satisfactory evaluation of the response.

This model is now used to simulate experimental band profiles resulting from more or less diluted molasses loads.

3. Experimental

The resin used in the experiments was Dowex C326 purchased from Dow Chemical; it is a sulphonated styrene–divinylbenzene cation-exchange resin of the gel type. The cross-linking is 6% and the mean diameter of the beads is 326 μm.

Softened beet molasses was furnished by Applexion. Softening is a necessary preliminary step in the purification process because exclusion is much more efficient when the resin counter ion is monovalent and the resin has a stronger affinity for divalent than for monovalent cations.

In order to simulate as closely as possible industrial operating conditions and especially to ensure that the ionic form of the resin is in equilibrium with the molasses ionic composition, a large amount of molasses was allowed to

percolate through the resin bed; the bed was then washed and was ready to be used.

The experimental device on which elutions were carried out consisted of a jacketed glass column (1 m × 5 cm I.D.) furnished by Pignat. It was equipped with a piston allowing introduction of the feed solution exactly at the top of the resin through a PTFE frit. A purge line ensured that a perfect and non-delayed step signal could be achieved at the entrance of the bed. Feed solutions and water used for rinsing were pumped from a thermostated bath at 70°C by a Gilson Minipuls peristaltic pump. All experiments were performed at 70°C and at a constant flow-rate of about 36 ml/min.

Molasses elution curves were obtained from the rectangular injection of 210 ml of more or less diluted molasses (the injection size corresponds to about 10% of the bed volume); the highest concentration tested corresponded to a molasses diluted twice, comparable to concentrations involved in industrial applications. Samples were collected with a Gilson 201 fraction collector and analysed according to the official methods recommended in the sugar industry for molasses analysis [9]: the sucrose concentration was determined by polarimetry after precipitation by lead acetate and ash was measured by conductimetry after dilution.

The results are related to the normalized time t/t_0, where t_0 is the mean residence time of a non-adsorbing tracer; it was evaluated from Blue Dextran breakthrough curves, as Blue Dextran has proved in previous work [10] to be a good external tracer; its concentration was measured by spectrophotometry with a Carl Zeiss PMQ II spectrophotometer at a wavelength of 635 nm.

Table 2 gives the operating conditions for each elution.

4. Results and discussion

The results obtained are fairly satisfactory (Fig. 3). However, in both cases considered (runs 1 and 2), the simulation overestimates the maximum of the sucrose peak and the steepness of the rear part and makes ash leave the column later than in experiments. As the general features are correctly predicted, however, we tried to improve the quality of the simulation by modifying the isotherm parameters. Empirically, it can be seen that parameters a and a' influence mainly the peak positions and b and b' influence the peak asymmetry; although effective, the influence of d and d' is less easy to characterize. Isotherm parameters were then optimized using a simplex algorithm so that the model response matched the experimental band profiles obtained with the less concentrated molasses load (run 1). Optimized parameters are given in Table 3 and the resulting elution curves are shown in Fig. 4. It can be verified also from Fig. 5 that the parameters so obtained allow the model to simulate fairly well the experiment on a more concentrated molasses (run 2). It is worth noting that the new sucrose equilibrium isotherm is linear in the absence of any other compound ($b = 0$), and that mutual influences of sucrose and ash are lowered.

It is not surprising that we had to modify the isotherm coefficients to account for the sucrose and ash behaviour in such a complex medium as molasses. First, contrary to the simple system

Table 2
Operating conditions for molasses elutions

Run No.	DM (g/l)	Sucrose (g/l)	Ash (g/l)	L (cm)	Injection size (min)	Q (ml/min)	ε	t_0 (min)
1	157	98.3	17.7	110.7	5.86	35.5	0.39	23.88
2	320	196.8	36.1	112.2	5.86	35.5	0.38	23.58
3	476	288.6	51.0	109.8	5.86	35.8	0.39	23.49

Fig. 4. Molasses elution curves (run 1): experiment (points) and best fit obtained with the simple equilibrium model (solid line).
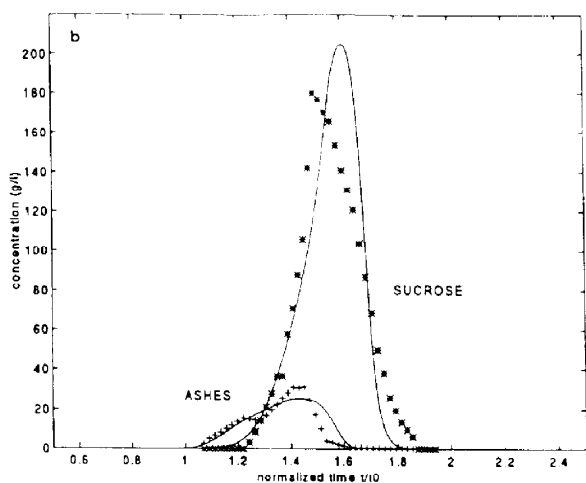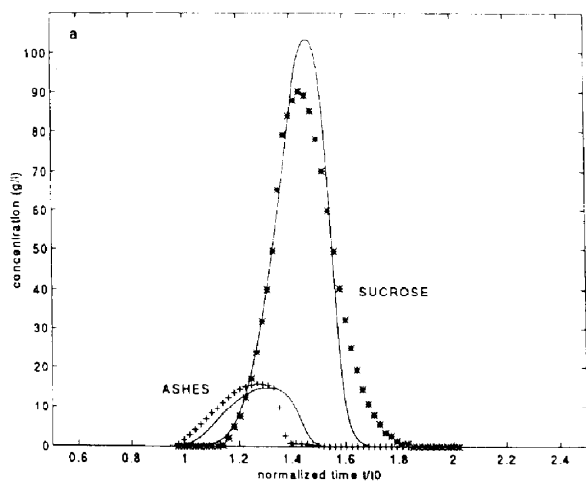

Fig. 3. Molasses elution curves: experiment (points) and simulation (solid line) by the simple equilibrium model with isotherm parameters measured on the sucrose–NaCl system. Operating conditions in Table 2. (a) Run 1; (b) run 2.
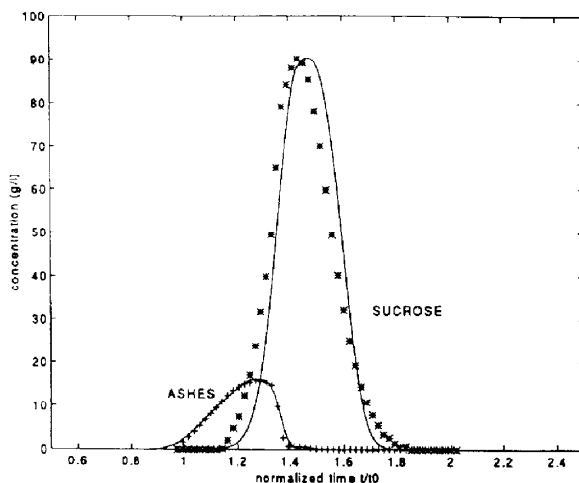
sucrose–NaCl–Na$^+$ resin, which served as a basis for modelling, ion exchange occurs: the actual ionic form of the resin results from an equilibrium with the molasses ionic composition during the elution; it is roughly estimated that about two thirds of the resin is converted into the K$^+$ form. Fig. 6 shows the influence of the ionic form of the resin (Na$^+$ and $\frac{1}{3}$Na$^+$/$\frac{2}{3}$K$^+$ resulting from equilibrium with molasses) on the adsorption of pure sucrose solutions at different concentrations: replacing even partially Na$^+$ with K$^+$ increases the sucrose retention significantly. Moreover, it should not be forgotten that

Table 3
Isotherm parameters obtained by frontal analysis of sucrose–NaCl mixtures and by fitting the simple equilibrium model with the molasses elution curve (run 1)

Method	Sucrose			Ash		
	a	b	d	a'	b'	d'
Measured by frontal analysis on sucrose–NaCl mixtures[a]	0.167	$0.307 \cdot 10^{-3}$	$0.172 \cdot 10^{-2}$	0.068	$0.176 \cdot 10^{-2}$	$0.293 \cdot 10^{-3}$
Fitted on molasses elution (run 1)	0.24	0.0	$0.172 \cdot 10^{-2}$	0.0134	$0.4 \cdot 10^{-2}$	$0.05 \cdot 10^{-3}$

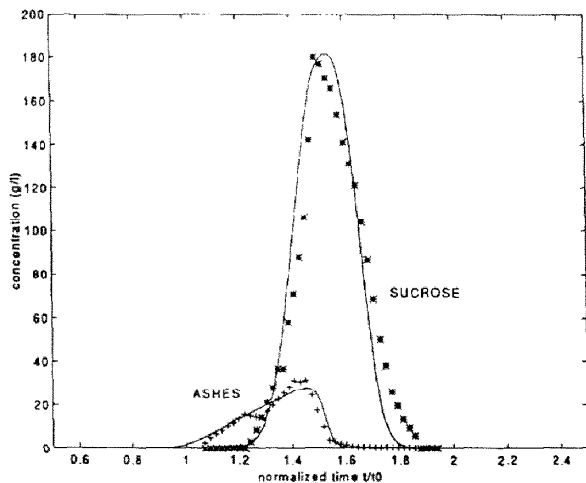[a] From Lewandowski and Lameloise [8].

Fig. 5. Molasses elution curves (run 2): experiment (points) and simulation (solid line) by the simple equilibrium model with isotherm parameters optimized on run 1.
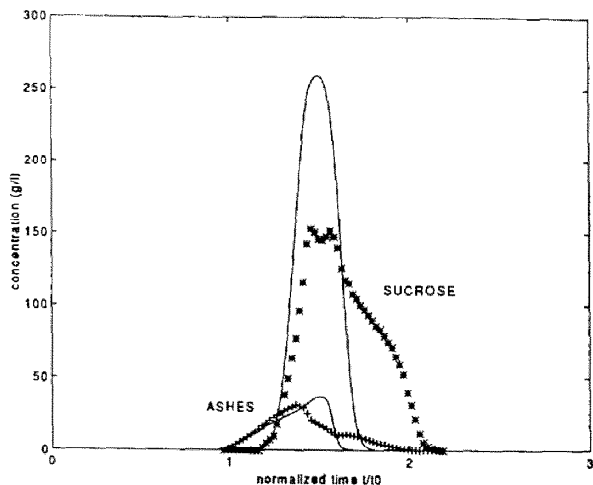

Fig. 7. Molasses elution curves (run 3): experiment (points) and simulation (solid line) by the simple equilibrium model with isotherm parameters optimized on run 1.

coloured matter, organic compounds such as betaine and other impurities contained in molasses may influence the sucrose and ash adsorption.

At higher concentrations of molasses (run 3: 288.6 g sucrose/l), modifications of the band profiles occur (Fig. 7): they broaden and flatten out, and a shoulder appears on the rear part of the band, almost visible on the sucrose peak. Simulation with previously optimized parameters

gives very poor results. Such deformations have also been observed when eluting highly concentrated sucrose–NaCl mixtures; therefore, they are not to be attributed to the influence of impurities in molasses such as betaine or coloured matter. At such concentration levels, mass transfer resistance is perhaps no longer negligible. A model accounting for sucrose transfer resistance was elaborated.

4.1. Mass transfer resistance model

As indicated by Ruthven [11], under most practically realizable conditions, the intraparticle resistance is more important than film resistance in determining the mass transfer rate. Therefore, film resistance was neglected.

As a gel-type resin was used here, a diffusion model characterized by an equivalent diffusivity D_e has a reasonable chance of describing sucrose migration inside resin beads. To avoid complexities rising from the second-order derivatives, the diffusion equation is often approximated by a linear driving force model with a mass transfer coefficient k_d. Glueckauf [12] has demonstrated the equivalence of the two models when isotherms are linear, provided $k_d = 5(D_e/R_p)$. Ruthven [11] showed that this equivalence is still
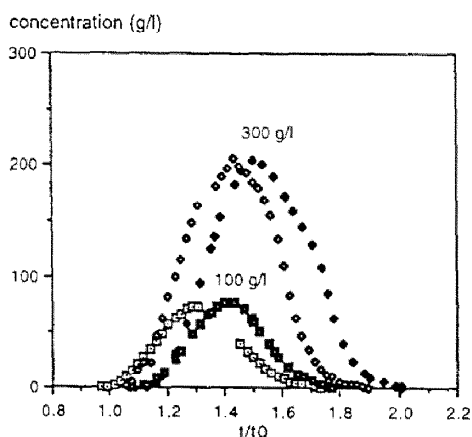

Fig. 6. Influence of ionic form of the resin on sucrose adsorption. Sucrose 100 g/l; resin in (□) Na⁺ form and (■) Na⁺/K⁺ form. Sucrose 300 g/l: resin in (◇) Na⁺ form and (◆) Na⁺/K⁺ form. Other operating conditions as in Table 2.

acceptable in the case of unfavourable or moderately favourable isotherms.

The following system is then to be solved:

$$u \cdot \frac{\partial c_1}{\partial z} + \frac{\partial c_1}{\partial t} + \frac{(1-\varepsilon)}{\varepsilon} \cdot \frac{\partial q_1}{\partial t} = 0 \qquad (16)$$

$$u \cdot \frac{\partial c_2}{\partial z} + \frac{\partial c_2}{\partial t} + \frac{(1-\varepsilon)}{\varepsilon} \cdot \frac{\partial q_2}{\partial t} = 0 \qquad (17)$$

$$\frac{\partial q_1}{\partial t} = \frac{1}{t_m}(q_1^* - q_1) \quad \text{with } t_m = \frac{R_p}{3k_d} \qquad (18)$$

Sucrose:

$$q_1^* = ac_1 + bc_1^2 + dc_1c_2 \qquad (19)$$

Ash:

$$q_2 = a'c_2 + b'c_2^2 + d'c_1c_2 \qquad (20)$$

Adopting the same discretization schemes as previously, a set of three equations with three unknowns is obtained and solved iteratively from boundary and initial conditions:

$$c_1(x, \tau + \Delta\tau)E + q_1(x, \tau + \Delta\tau)F + G = 0 \qquad (21)$$
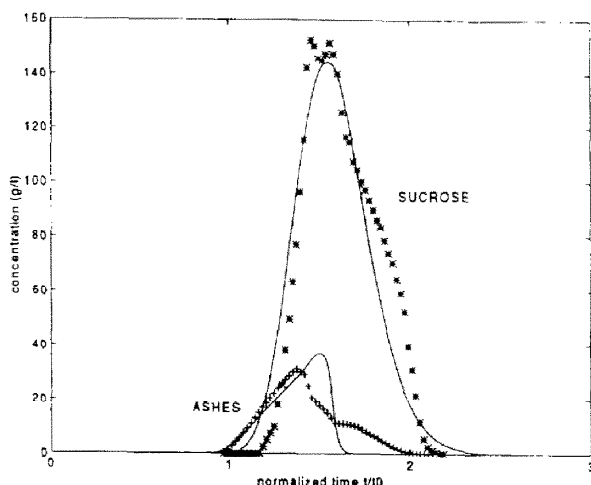
$$q_1(x, \tau + \Delta\tau)H + T = 0 \qquad (22)$$

Fig. 8. Molasses elution curves (run 3): experiment (points) and best fit obtained with the mass transfer resistance model (solid line).

$$c_2(x, \tau + \Delta\tau)U + c_1(x, \tau + \Delta\tau)V + W = 0 \qquad (23)$$

This model with a time constant $t_m = 50$ s improves the sucrose representation and especially the band broadening, but without accounting for the shoulder (Fig. 8). Moreover, the first coefficient of the isotherm has to be increased ($a = 0.3$ in place of 0.24) to locate the band at the correct position, suggesting that the shape of the isotherm might be more complex at these concentrations. Finally, no significant improvement to the ash band profile is observed. At high concentration, as exclusion is less effective, penetration of ash into the resin beads is no longer negligible, and kinetic limitation of transfer should probably also be considered.

5. Conclusion

For loads representing 10% of the bed volume, a simple equilibrium model based on sucrose and NaCl isotherms gives a satisfactory representation of the elution of molasses containing up to 320 g DM/l (which corresponds to a dilution ratio of about 3); a minor adjustment of parameters is necessary, however, to take into account the influence of the ionic form of the resin and the more complex nature of the medium.

For a more concentrated load, the predictions of the simple equilibrium model are far from reality. The introduction of a resistance to sucrose transfer in the form of a linear driving force allows the sucrose representation to be improved, but does not account for the shoulder on the rear side of the sucrose band and for ash tailing. In order to ensure continuity between the two models, the kinetic parameter should vary with concentration. Moreover, the necessary modification of the sucrose isotherm first parameter to locate the peak at the right position suggests that the isotherm might be more sophisticated at these concentrations.

However, as far as batch-type experiments are concerned, optimization of purity and recovery of the sucrose fraction would rather lead to the choice of a limited load with low concentration.

Symbols

a, a'	isotherm coefficient
b, b'	isotherm coefficient
c	concentration in the liquid phase
d, d'	isotherm coefficient
D_e	effective diffusivity
k_d	mass transfer coefficient
L	bed length
q	concentration in solid phase (averaged over particle volume)
q^*	concentration in the solid phase, at the particle surface
Q	flow-rate
R_p	particle radius
S	column section
t	time
t_0	mean residence time of a non-adsorbing tracer
t_m	transfer time constant
u	velocity
x	dimensionless abcissa in column
z	abcissa in column

Greek letters

ε	external porosity
τ	normalized time $= t/t_0$
τ_e	normalized injection time

Subscripts

1	relates to sucrose
2	relates to NaCl or ash

Abbreviations

DM	dry matter
SMB	simulated moving bed

References

[1] M. Buckley and G. Norton, Int. Sugar J., 93 (1991) 204.
[2] K.P. Chertudi, Int. Sugar J., 93 (1991) 28.
[3] R. Gadomski, Sugar Azucar, (1991) 34.
[4] M. Kearney, in Proceedings of the Sugar Processing Research Conference, 1990, p. 291.
[5] G. Hotier, in Proceedings of the 9th International Symposium on Preparative and Industrial Chromatography, Nancy, April 1992, p. 235.
[6] B.P. Baker, Composition, Properties and Uses of Molasses and Related Products, United Molasses Trading, 1971.
[7] M. Saska, M.D. Wu, S.J. Clarke, K. Iqbal and M. Mrini, Int. Sugar J., 95 (1993) 137.
[8] R. Lewandowski and M.L. Lameloise, Chem. Eng. Proc., 31 (1992) 207.
[9] Méthodes d'Analyses de l'I.R.I.S., Institut de Recherche de l'Industrie Sucrière, Villeneuve d'Ascq, 1984.
[10] M.L. Lameloise and V. Viard, J. Chromatogr. A, 679 (1994) 255.
[11] D.M. Ruthven, Principles of Adsorption and Adsorption Processes, Wiley, New York, 1984.
[12] E. Glueckauf, Trans. Faraday Soc., 51 (1955) 1540.